

# The use of spherical coordinates in the interpretation of seismograms

Anthony J. Lomax and Alberto Michelini

Seismographic Station, Department of Geology and Geophysics, University of California, Berkeley, CA 94720, USA

Accepted 1987 October 14. Received 1987 October 12; in original form 1987 June 12

## SUMMARY

In this paper we describe the use of spherical coordinates and lower hemisphere, equal-area projection to display and interpret seismograms. Information from three-component seismometers displayed in spherical coordinates and on an equal-area projection shows particle motion more clearly than do displays in Cartesian rectangular coordinates. In the spherical coordinate system characteristic patterns such as square waves and triangular waves simplify the identification of wave types on seismic records. The use of spherical coordinates is a simple method for increased comprehension of the particle motion, wave polarizations and phase onsets in a seismic record.

**Key words:** Cartesian coordinates, particle motion, polarization analysis, seismograms, spherical coordinates

## INTRODUCTION

A basic problem in instrumental seismology is to represent graphically the ground motion at a point caused by the passing of seismic waves. Three-component seismograms represent the particle motion of this point in 3-D space and time. The changes in amplitude and direction of this motion indicate the arrival times of seismic phases, the type and polarization of wave motion, the direction of wave arrival and other wave parameters (e.g. Aki & Richards 1980; Bullen & Bolt 1985). The direct output of most three-component seismometers represents motions in Cartesian rectangular coordinates because these instruments measure linear motions along orthogonal axes. But since the appearance of seismograms displayed in rectangular coordinates is dependent on the orientation of the three axes, the vector amplitude and polarization of the particle motion may be obscured.

Transformations of the ground motion that emphasize amplitude and direction information would greatly benefit seismogram analysis. The aim of transformations, common in time series analysis, is to present the data in a form that gives greater weight to the most desired information. Typically this is done with a change of coordinate system or reference frame. It is found that data interpretation from different perspectives often results in the discovery of relationships not otherwise evident (e.g. Taner, Koehler & Sheriff 1979). Examples of such transformations include the Fourier transform (e.g. Bracewell 1965), complex trace analysis (e.g. Farnbach 1975; Taner *et al.* 1979), axis rotations (e.g. radial and transverse components of the particle motion with respect to source receiver azimuth). All of these transformations can be defined as *reversible*. That is, they involve no loss or averaging of the data. The original data set can be recovered by the appropriate reverse transformation.

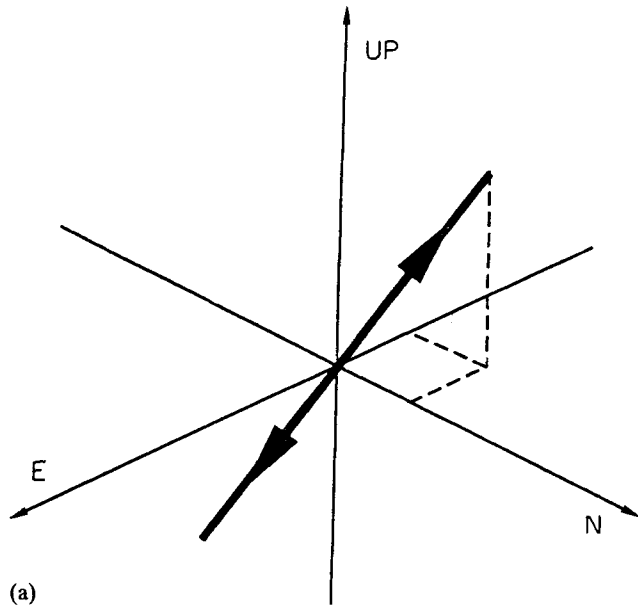
Wavefields recorded at a three-component seismometer

can be analysed using polarization analyses (e.g. Kanasevich 1981, for a review; Matsumara 1981; Plesinger, Hellweg & Seidl 1986; Vidale 1986). These methods tend to use *non-reversible* transformations that resolve dominant polarization states of the wavefield. In this paper, however, we propose the use of a direct, reversible transformation of the time series to spherical coordinates for graphical analysis by the user.

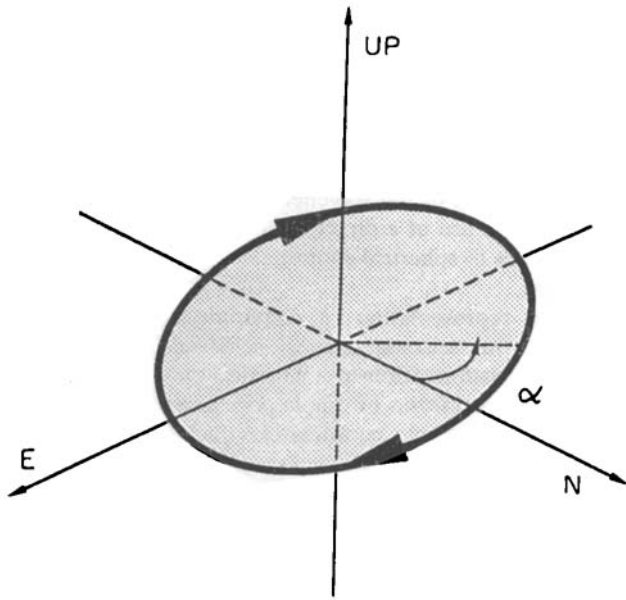
A useful representation of amplitude and polarization information in seismograms is achieved by a simple coordinate transformation to a spherical coordinate system. The mathematical forms of simple polarized waves are much simpler in spherical coordinates than in rectangular coordinates, so that plots in spherical coordinates display polarization information more concisely. It follows that with spherical coordinates the characteristics of particle motion are more easily identified, regardless of the directions of polarization or wave arrival. In addition, a separate display of the three spherical coordinates using a lower hemisphere, equal-area projection allows the unambiguous representation of particle position in space on one plot. If this plot is generated by animation on a computer graphics system, all four dimensions of particle motion, including time, can be viewed.

## CARTESIAN COORDINATES

In the Cartesian coordinate system, the position of a point is represented by its projection on to three orthogonal axes (Figs 1 and 2a). For seismograms, these axes usually correspond to the orientation of the seismic sensors or to the vertical and the directions radial and transverse to the epicentre. In general, as the position of the point moves, its projections on all three axes will change, splitting the information of the motion into three parts. Because of this splitting, displays in rectangular coordinates to resolve particle motion require mental synthesis of all three



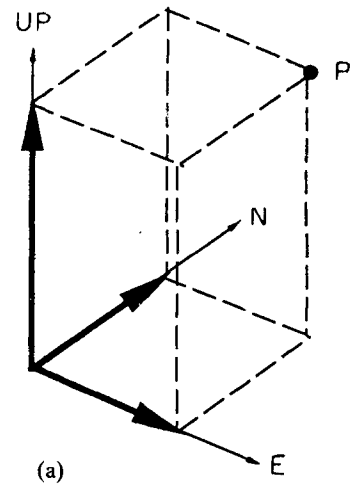
(a)



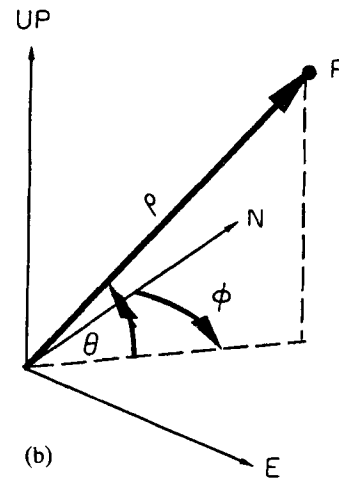
(b)

**Figure 1.** Examples of particle motion trajectories: (a) linearly polarized; (b) elliptically polarized.

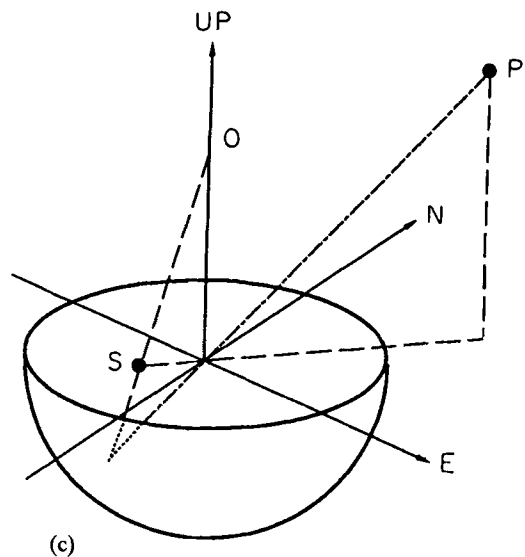
components of motion. As an example, consider several cycles of sinusoidal, linearly polarized motion along a line that is not parallel to any of the coordinate axes (Fig. 1a). In rectangular coordinates, this motion will project as a sinusoid on each of three axes (Fig. 3a). Construction of the complete particle motion from this display requires calculations using the relative amplitudes and phases of the sinusoids. For this reason, important details such as strong polarization for only a fraction of a cycle, might be completely overlooked on the rectangular coordinate display.



(a)



(b)



(c)

**Figure 2.** Coordinate system representation of a point  $P$ : (a) Cartesian rectangular coordinates; (b) spherical coordinates and (c) projection of  $P$  on to a lower hemisphere projection.  $S$  is the projection of  $P$  on to the horizontal plane of the projection.

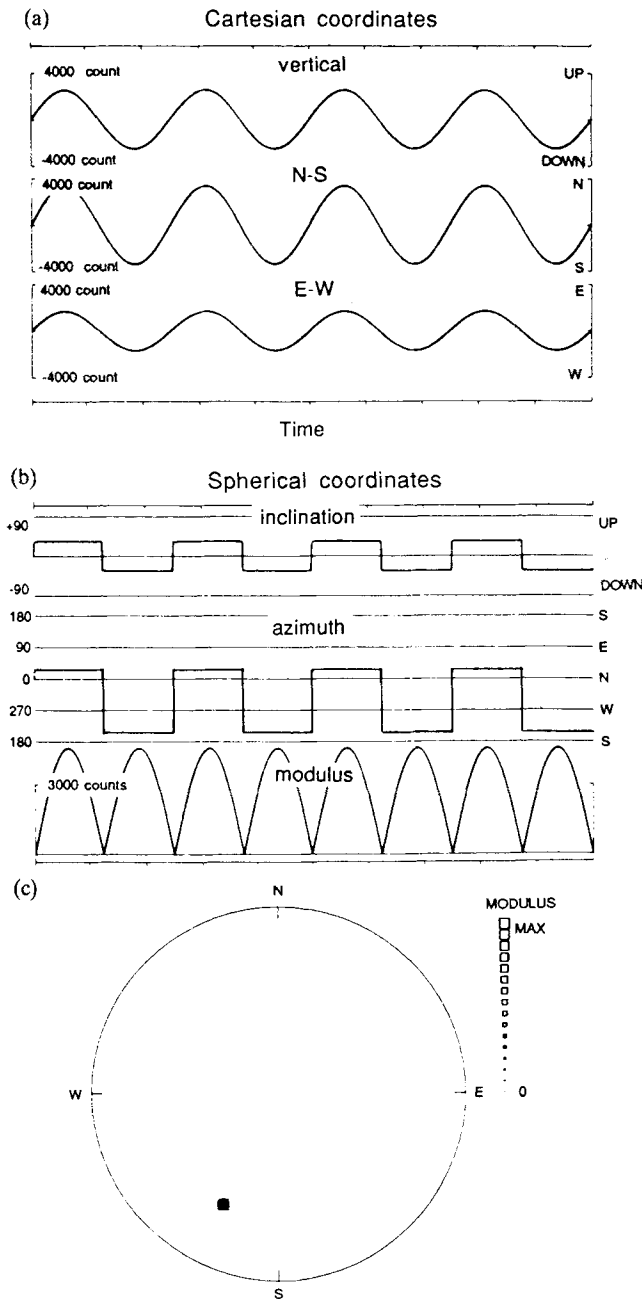


**Figure 3.** Linearly polarized synthetic seismogram of sinusoidal particle motion. (a) Display in Cartesian coordinates; (b) display in spherical coordinates. The inclination,  $\theta$ , is measured from the horizontal ( $-90^\circ \leq \theta \leq 90^\circ$ ); the azimuth,  $\phi$ , lies on the horizontal plane ( $0^\circ \leq \phi < 360^\circ$ ). (c) Display on a lower hemisphere equal-area projection with the symbol size proportional to the modulus,  $\rho$ , of the radius vector.

### SPHERICAL COORDINATES

In the spherical coordinate system the position of a point  $P$ , is specified by the *radius vector* from the origin to the point (Fig. 2b). We define the three coordinates as: (1) the length or *modulus*,  $\rho$ , of the radius vector; (2) the *inclination*,  $\theta$ , of this vector above or below the horizontal plane; and (3) the *azimuth*,  $\phi$ , clockwise from north of the projection of the radius vector on the horizontal. For a point with position

$P[Z(t), N(t), E(t)]$  in Cartesian coordinates, the modulus is

$$\rho(t) = [Z(t)^2 + N(t)^2 + E(t)^2]^{1/2}$$

the inclination [ $-90^\circ \leq \theta(t) \leq +90^\circ$ ] is

$$\theta(t) = \sin^{-1} [Z(t)/\rho(t)],$$

and the azimuth  $\phi$  [ $0^\circ \leq \phi(t) < 360^\circ$ ] is

$$\phi(t) = \tan^{-1} [N(t)/E(t)].$$

The value of  $\phi$  is given a range of  $360^\circ$  by adding  $180^\circ$  to  $\phi$  if  $E(t) < 0$ . The angles  $\theta$  and  $\phi$  are undefined when  $\rho = 0$ , and can be unstable or discontinuous for  $\rho$  small.  $\phi$  is also undefined when  $\theta = \pm 90^\circ$ .

We may now consider the previous example of linearly polarized particle motion (Fig. 1a), displayed in spherical coordinates. As the particle moves away from the origin and returns,  $\rho$  changes from zero to a maximum and back to zero. During this half cycle, the  $\theta$  and  $\phi$  are constant (Fig. 3b). When the particle passes through the origin,  $O$ ,  $\rho = 0$ , the inclination jumps to the negative of its value and the azimuth jumps  $180^\circ$  (Fig. 3b). This motion appears in the form of a *square wave* on the inclination and azimuth plots and as positive, half sinusoid cycles on the modulus plot (Fig. 3b). The type of polarization can be determined from these displayed patterns, even if the motion is well polarized for only a fraction of a cycle. If the polarization is linear, as in this example, its orientation can be read directly from the constant values on the inclination and azimuth plots. One should note that it is necessary to pay attention to removing any constant or long-period, non-zero baseline from the three-component recordings before applying the spherical coordinate transformation. If this offset is not removed, shifts in the values of the spherical coordinates will occur.

### EQUAL-AREA LOWER HEMISPHERE PROJECTION

Vector representation in 3-D space is conveniently represented by lower hemisphere equal-area projections (see Aki & Richards 1980; Ragan 1973). On these projections, a line through the origin is represented as a point and a plane through the origin as an arc.

For the corresponding display of a seismogram, information from the three spherical coordinates can be combined by the use of a lower hemisphere, equal-area projection (Fig. 2c). We plot a symbol at the point on the projection representing the orientation of the line containing the radius vector at each sequential time increment. The symbol size is made proportional to the modulus,  $\rho$ , of the radius vector.

All the digital samples of an ideal, linearly polarized wave (such as  $P$  or  $S$  in homogeneous, isotropic elastic media) will plot at the point on the projection corresponding to the inclination and azimuth of the line of the particle motion (Fig. 3c). During more complicated particle motions, the grouping of a number of samples at one location indicates temporary linearly polarized particle motion. The orientation of polarization is shown directly by the location of this grouping on the projection.

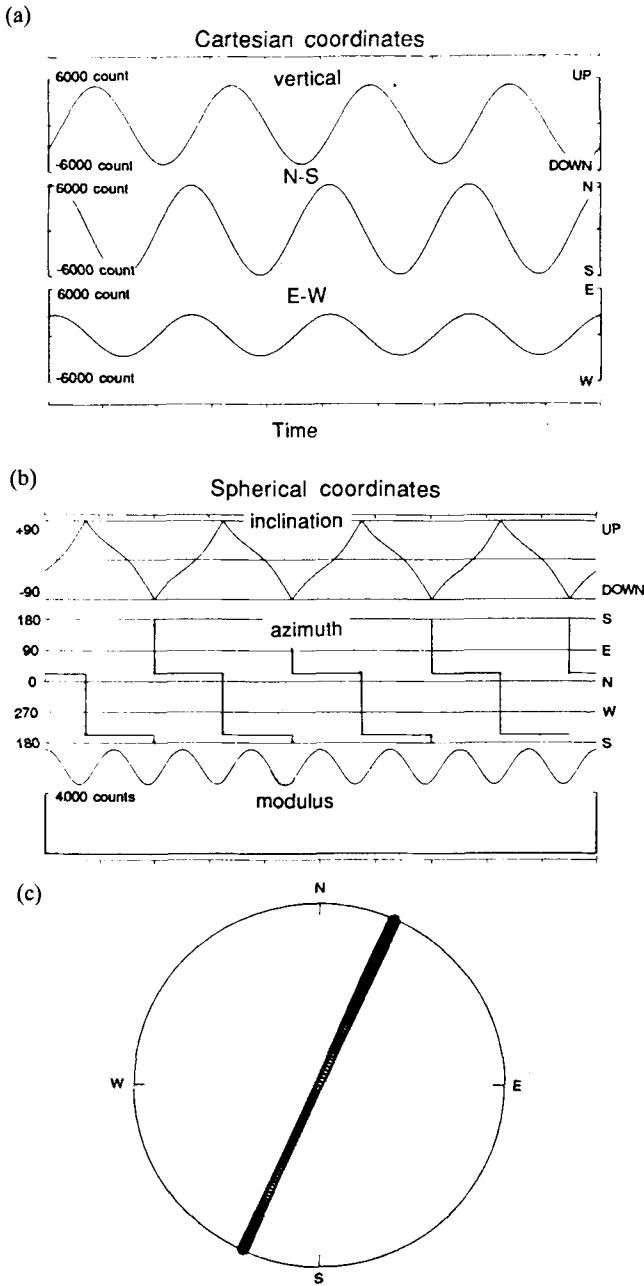


**Figure 4.** Elliptically polarized synthetic seismogram of particle motion lying on a vertical plane. The axes of the ellipse have a 3:2 ratio. (a), (b) and (c) are as in Fig. 3.

**ELLIPTICALLY POLARIZED WAVES**

In elliptically polarized motion (such as Rayleigh wave motion in an isotropic, homogeneous half-space) a ground particle moves in general along an ellipse in some plane containing the origin and never passes through the origin (Fig. 1b). The superposition of two out-of-phase, linearly polarized waves can also produce elliptically polarized particle motion.

In Cartesian coordinates an elliptically polarized wave will plot in the form of a sine wave on each coordinate (Figs 4a and 5a). Since the waveform pattern for elliptical motion may be similar to that of linearly polarized motion, the two

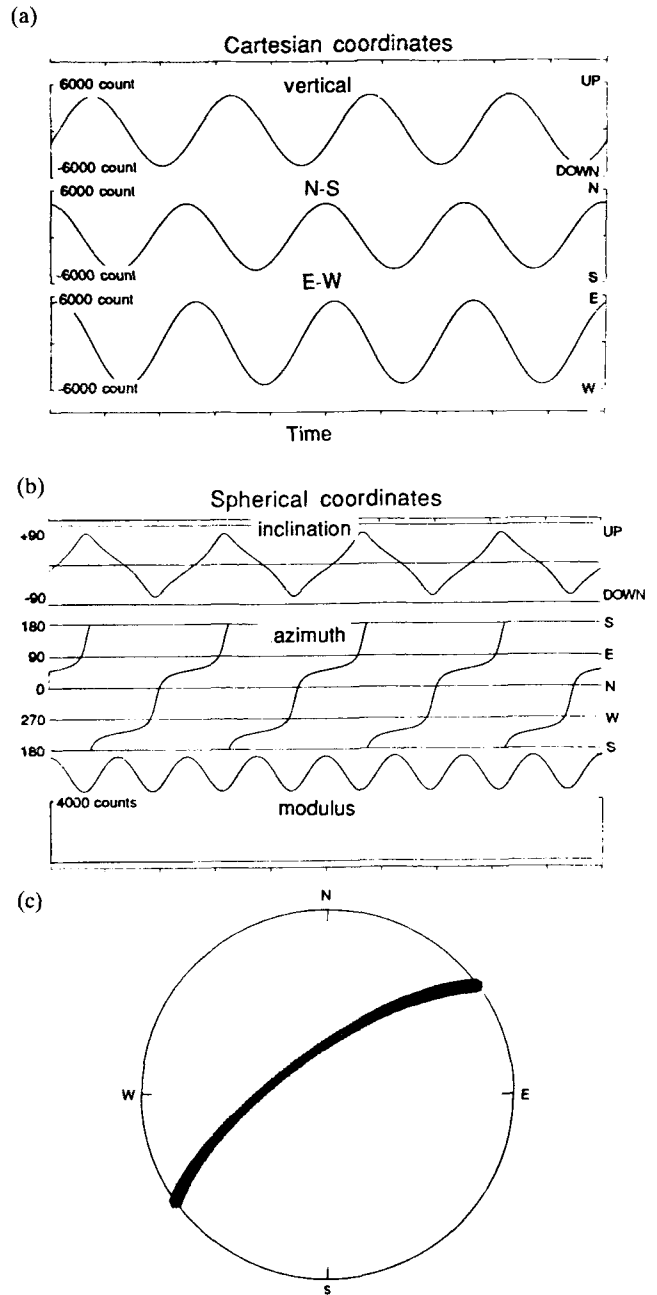


**Figure 5.** Elliptically polarized synthetic seismogram of particle motion on a plane dipping approximately 70° from the horizontal. (a), (b) and (c) are as in Fig. 3.

patterns of polarization may be not easily distinguished in rectangular coordinates. Also, the plane of elliptical polarization cannot easily be determined in rectangular coordinates unless it is coincident with two of the coordinate axes.

Because, in general, the particle does not pass through the origin, elliptically polarized motion is characterized by a non-zero modulus,  $\rho$ , in spherical coordinates. If the motion lies in a vertical plane, then it plots in the form of a *triangular wave* in inclination that peaks at 90° and -90° (Fig. 4b); the azimuth plot will have the form of a *square wave* (Fig. 4b). The discontinuities in the azimuth plot correspond to jumps of 180° as the particle motion passes

over and under the origin. If the plane of motion tilts away from the vertical (as with waves in anisotropic media, e.g. Kirkwood & Crampin 1981) the inclination triangular wave peaks at less than  $\pm 90^\circ$  and the azimuthal square wave pattern distorts into a sloping square wave (Fig. 5b). When the motion is entirely in the horizontal plane, the inclination triangle wave degenerates to a line at  $0^\circ$  but the azimuth plot may still exhibit sloping square waves. If the motion is circular, however, the azimuth plot will show diagonal lines of constant slope, indicating a constant change of azimuth with time.

On the equal-area projection, elliptical particle motion plots as an arc corresponding to the projection of the plane of motion on the lower hemisphere. In the case of a vertical plane of motion, this arc is a straight line through the centre of the plot in the direction of the strike of the plane of motion (Fig. 4c). For tilted, elliptical ground motion, the projection is an arc that intersects the outer edge of the plot at the direction of the strike of the plane of motion. The amount of tilting is given by the inclination at the point where the arc is nearest the centre of the plot (Fig. 5c).

### EXAMPLES

We illustrate the use of spherical coordinates for seismogram analysis with the Berkeley ultra-long period, broadband records of the Kermadec Islands Earthquake of 1986 October 20. This event ( $M_s = 8.3$ ) occurred at a distance of about  $85^\circ$  SW of Berkeley at shallow depth.

Figure 6 shows a 3-min window of the S group arrivals from the Kermadec event. From expected travel times (Jeffreys–Bullen), pulse 1 is associated with the S and SKS phases, and the larger pulses 2 and 3 are associated with the PS and perhaps PPS phases. Pulse 3 is followed by a small wave train denoted by 4.

On the rectangular coordinate plot (Fig. 6a), the trace of pulse 1 appears on all three components and consequently the recognition of its polarization requires separate calculation. On the spherical coordinate plot (Fig. 6b), however, this pulse shows the half sine wave modulus and the stable inclination and azimuth signature characteristic of a linearly polarized wave. The inclination read directly from this plot is approximately  $15^\circ$  above the horizontal and the azimuth is about  $10^\circ$  west of south. On the equal-area projection, (Fig. 6c), this pulse plots as a tight group of points at the location on the lower hemisphere corresponding to the upper hemisphere inclination and azimuth found above. Assuming wave propagation along great circle paths from hypocentre to receiver, the SH motion is normal to the vertical plane striking along the back azimuth while the SV motion recorded at the surface lies within this plane (e.g. Aki & Richards 1980; Bullen & Bolt 1985). Pulse 1, displaying a nearly horizontal inclination, would therefore correspond to the superposition of SH and SV waves. It should be noted that this is a measurement of S-wave polarization applicable to fault plane solutions.

Pulse 2 appears dominantly on the radial component and slightly on the vertical component of the rectangular coordinate plot (Fig. 6a). This pattern indicates nearly horizontal particle motion along the direction radial to the epicentre. On the spherical coordinate plot and the equal area projection (Fig. 6b and c), this motion is clearly read

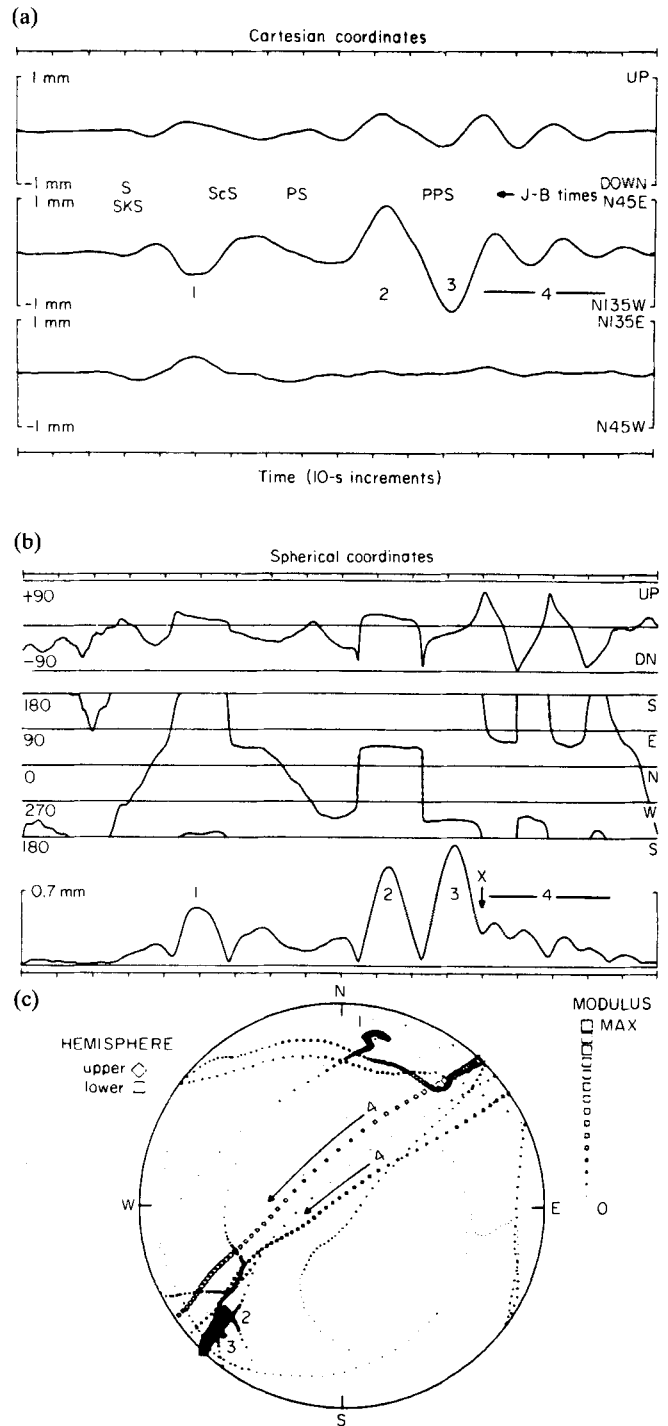


**Figure 6.** 3-min window for the S arrival phases of the Kermadec Earthquake (1986 October 20,  $M_s = 8.3$ ) recorded at Berkeley (BKS) by an Ultra Long Period instrument. (a) (b) and (c) are as in Fig. 3. Approximate Jeffreys–Bullen arrival times are shown in (a).

as to be strongly linearly polarized with a SW azimuth and inclination of nearly  $20^\circ$  below the horizontal. Pulse 3 exhibits the same polarization as pulse 2 with particle motion on the opposite side of the origin. Since the particle motion of these pulses lies close to the radial plane, these waves must be superposition of P- and SV-type motion,

perhaps due to the *PS* and *SP* phase arrivals. This is likely since no *SH* motion is expected in *PS* and *SP* arrivals in a spherically symmetric Earth.

Immediately following pulse 3 is an elliptically polarized wave 4, indicated on the spherical plot (Fig. 6b), by a triangle pattern in inclination, a square wave in azimuth and a positive modulus. Though the onset of this phase is difficult to identify on the Cartesian coordinate plot (Fig. 6a), it is indicated by a distinct change in pattern at the point *X* on the spherical coordinate plot (Fig. 6b). The digital samples of this arrival fall along an arc on the equal-area projection and move from NE to SW on the lower hemisphere, indicating prograde Rayleigh motion. We thus interpret this arrival to be a surface wave of PL type (Oliver & Major 1960) generated near the receiver by the interaction of the *PS* and *PPS* waves and the Earth's surface.

The plots in Fig. 7 show a 3-min window of the Rayleigh wave train from the Kermadec event. The Cartesian coordinate plot (Fig. 7a) shows the motion mostly on the vertical and radial components, though there is some motion on the transverse components. It is not clear from this plot whether particle motion out of the radial plane or out of the vertical plane is causing the motion on the transverse component. The spherical coordinate plot (Fig. 7b) shows non zero modulus and approximate square wave azimuth and triangle wave inclination variations characteristic of elliptically polarized waves. The inclination peaks at less than  $90^\circ$ , however, and the azimuth plot shows sloped peaks and troughs, indicating that the particle motion is not in the vertical plane. This is shown most clearly on the equal area projection (Fig. 7c) where the particle motion defines an arc across the plot that passes to the SE of the centre of the projection with an inclination ranging between  $5^\circ$  and  $15^\circ$  from the vertical. The spherical plot and the lower hemisphere projection also show that the strike of the orbit is approximately coincident with the radial direction ( $S40^\circ W$ ). In addition, the tilting of the ground particle orbits might be explained by 'Tilted Rayleigh' (Crampin 1975) motion produced by anisotropy in the oceanic lithosphere or by the interaction of the surface waves with a somewhat complex ocean-continent boundary. A complete interpretation is outside the scope of this paper but the advantages of the identification of anomalous particle motions using spherical coordinates and the lower hemisphere projection are clear.

In the final example, we show the use of the radius vector modulus of the spherical coordinates transformation of a local earthquake recording (Fig. 8). The earthquake occurred in Bear Valley, Central California on 1987 March 11 ( $M_L = 2.7$ ) and was recorded by the three-component, digital, broadband station at Mount Hamilton at a distance of approximately 100 km. In spherical coordinates (Fig. 8b), the *P* and *S* phase arrivals onsets and coda shapes are clearer compared to those on the Cartesian coordinates display (Fig. 8a). This advantage is a result of the decoupling of orientation and modulus information obtained through the spherical coordinate transformation. This example illustrates that the plot of modulus,  $\rho$ , may be particularly useful for automatic *P*, *S* selection and coda duration algorithms when three-component recordings are available but only one channel can be telemetered or processed.

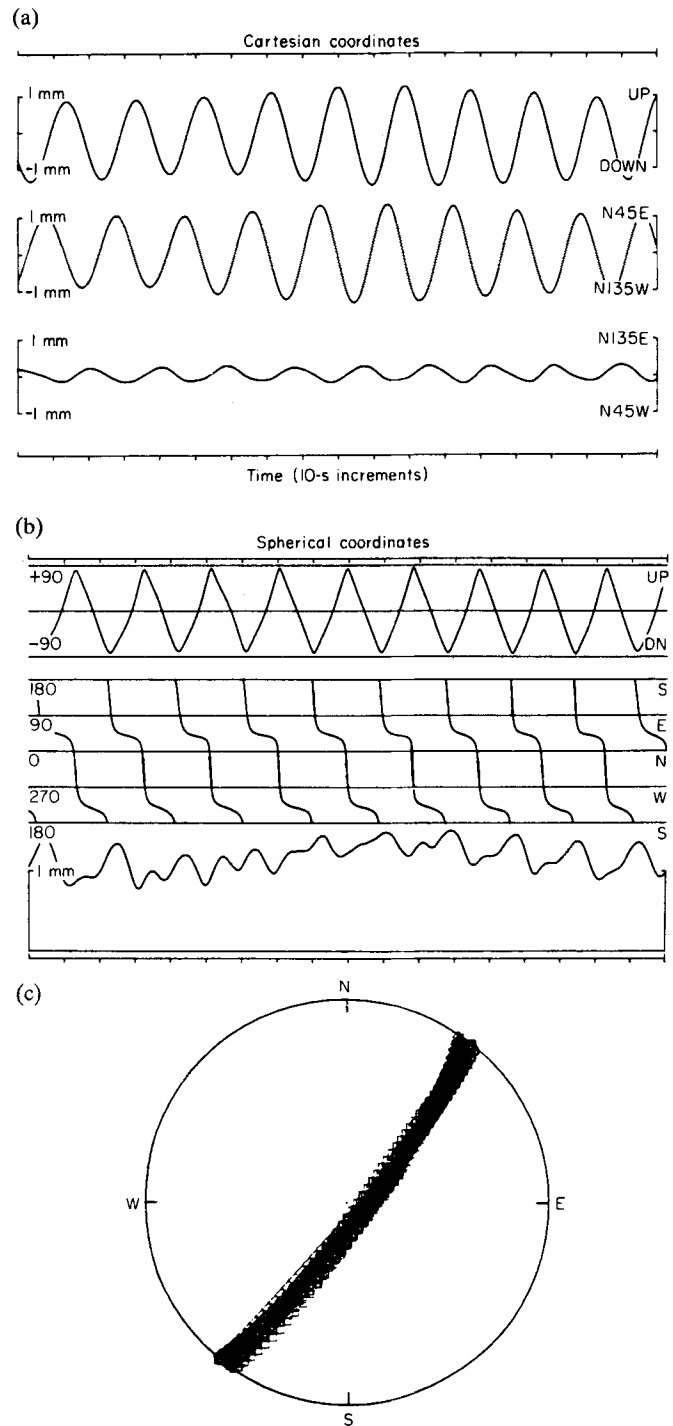
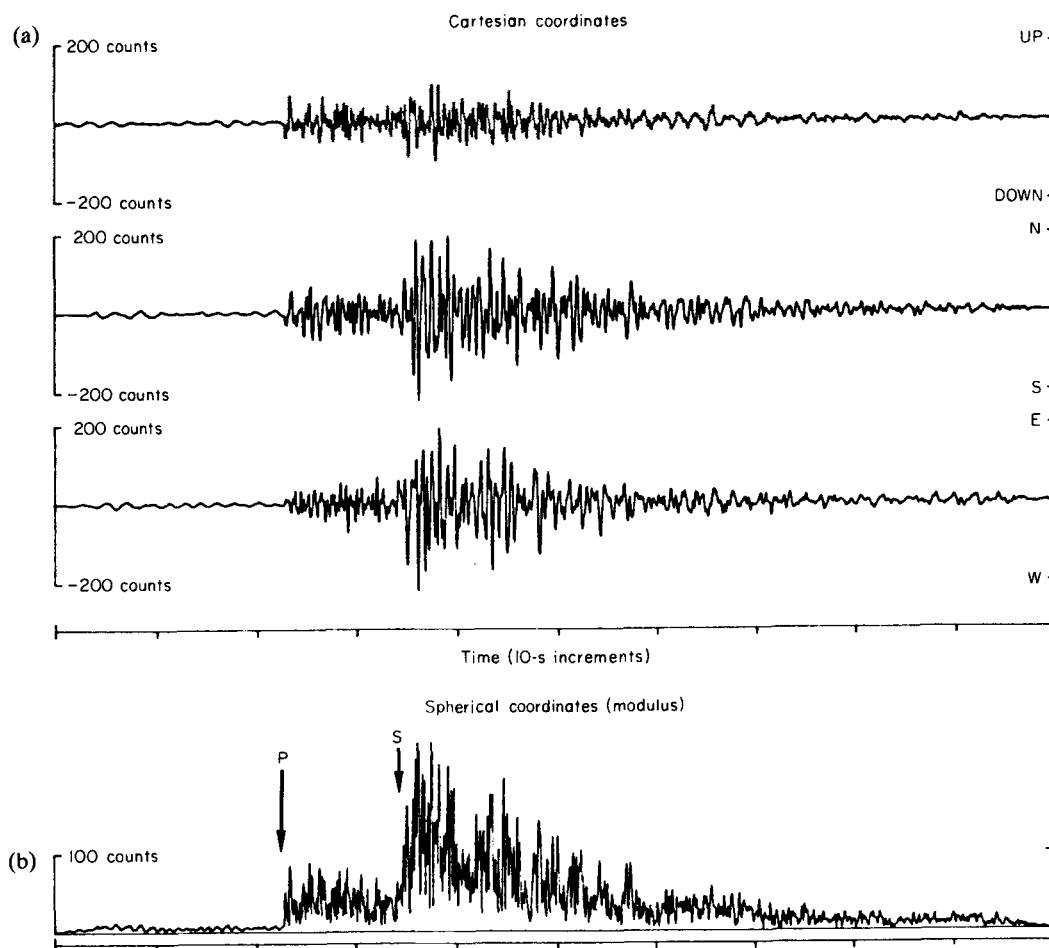


Figure 7. 3-min window of the Rayleigh surface wave train for the Kermadec Earthquake. (a), (b) and (c) as in Fig. 3.

## DISCUSSION

As the examples given above demonstrate, information from three-component seismometers displayed in spherical coordinates and on an equal-area lower hemisphere projection often show particle motion more clearly than do displays in Cartesian rectangular coordinates. This result follows because the mathematical equations for fundamental particle orbits, such as linear and elliptically polarized



**Figure 8.** Local earthquake recorded at Mount Hamilton, Central California, by a broadband, digital instrument. (a) Is as in Fig. 3; (b) modulus axis of the spherical coordinate display. The vertical lines are drawn on the  $P$  and  $S$  arrival times based on distinct increases of  $\rho$  above its previous values. These picks are compared with the Cartesian display (a). The azimuth and inclination plots are not shown because they are rather complex on this time scale.

motion, are simpler when expressed in spherical rather than in rectangular coordinates. The simpler forms lead to characteristic patterns, such as triangle and square waves, on seismograms displayed in spherical coordinates. Some of these patterns have already been pointed out by Vidale (1986) in his sophisticated polarization analysis. Our experimentation with recordings of ground motions indicates that these coordinates may also be useful in machine algorithms designed to discriminate between wave patterns in seismograms.

Once a direction of polarization is recognized, more traditional projections of particle orbits can be generated using this direction for the relevant section in the seismogram. We also suggest that the spherical coordinate transformation can be used as a valuable tool for studies of anisotropy and ray multipathing. The display methods discussed in this paper are relatively easy to implement on currently available micro-computer graphics systems, allowing enhanced recognition of particle position, phase onsets, wave polarization and changes in phase type without expensive computer hardware.

## ACKNOWLEDGMENTS

We thank Bruce Bolt and Thomas McEvilly for reviewing the paper, Robert Uhrhammer for suggestions in the early stages of this study and Walter Alvarez who kindly allowed us to use his word processing facilities. We also thank John Vidale and an anonymous reviewer for many helpful comments and suggestions. The research was supported by NSF (ECE 84-17856) and USGS (14-08-0001-G-723) grants.

## REFERENCES

- Aki, K. & Richards, P. G., 1980. *Quantitative Seismology, Theory and Methods*, 768 pp. W. H. Freeman and Co., San Francisco.
- Bracewell, R. N., 1965. *The Fourier Transform and its Applications*, 381 pp. McGraw-Hill Inc., New York.
- Bullen, K. E. & Bolt, B. A., 1985. *An Introduction to the theory of Seismology*. Cambridge University Press.
- Crampin, S., 1975. Distinctive particle motion of surface waves as diagnostic of anisotropic layering, *Geophys. J. R. astr. Soc.*, **40**, 177-186.
- Farnback, J. S., 1975. The complex envelope in seismic signal analysis, *Bull. seism. Soc. Am.*, **65**, 951-962.

- Kanasewich, E. R., 1981. *Time Sequence Analysis in Geophysics*, 480 pp. University of Alberta Press.
- Kirkwood, S. C. & Crampin, S., 1981. Surface wave propagation in an ocean basin with an anisotropic upper-mantle: numerical modelling, *Geophys. J. R. astr. Soc.*, **64**, 463–485.
- Matsumura, S., 1981. Three-dimensional expression of seismic particle motions by the trajectory ellipsoid and its application to the seismic data observed in the Kanto District, Japan, *J. Phys. Earth*, **29**, 221–239.
- Oliver, J. & Major, M., 1960. Leaking modes and the PL phase, *Bull. seism. Soc. Am.*, **50**, 165–180.
- Plesinger, A., Hellweg, M. & Seidl, D., 1986. Interactive high-resolution polarization analysis of broadband seismograms, *J. Geophys.*, **59**, 129–139.
- Ragan, D. M., 1973. *Structural Geology*. John Wiley, New York.
- Taner, M. T., Koehler, F. & Sheriff, R. E., 1979. Complex seismic trace analysis, *Geophys.*, **44**, 1041–1063.
- Vidale, J. E., 1986. Complex polarization analysis of particle motion, *Bull. seism. Soc. Am.*, **76**, 1393–1405.